Arthritis Research & Therapy

RESEARCH

Open Access

Distinct metabolic profiles of circulating plasmacytoid dendritic cells in systemic sclerosis patients stratified by clinical phenotypes

Beatriz H. Ferreira[1,2], Carolina Mazeda[3,4,5], Eduardo Dourado[3,4,6], João L. Simões[1,7], Ana Rita Prata[3,4], Rafael J. Argüello[8,9], Iola F. Duarte[2,10], Philippe Pierre[1,8,11] and Catarina R. Almeida[1*]

Abstract

Background Plasmacytoid dendritic cells (pDCs) play a key role in systemic sclerosis (SSc) pathophysiology. However, despite the recognised importance of metabolic reprogramming for pDC function, their metabolic profile in SSc remains to be elucidated. Thus, our study aimed to explore the metabolic profile of pDCs in SSc and their potential contribution to the disease.

Methods Peripheral blood mononuclear cells (PBMCs) were isolated from the blood of healthy donors and SSc patients. SCENITH™, a single-cell flow cytometry-based method, was applied to infer the metabolic profile of circulating pDCs from patients with SSc. pDCs ($CD304^+$ Lin^-) at steady-state or stimulated with CpG A were analysed. Toll-like receptor (TLR)9 activation was confirmed by ribosomal protein S6 phosphorylation.

Results Circulating pDCs from ten healthy donors and fourteen SSc patients were analysed. pDCs from anti-centromere antibody-positive (ACA^+) patients displayed higher mitochondrial dependence and lower glycolytic capacity than those from anti-topoisomerase I antibody-positive (ATA^+) patients. Furthermore, cells from both ACA^+ patients and limited cutaneous SSc (lcSSc) patients showed a stronger response towards TLR9 activation than cells from ATA^+, anti-RNA polymerase III antibody-positive (ARA^+) or diffuse cutaneous SSc (dcSSc) patients.

Conclusions An innovative single cell flow cytometry-based methodology was applied to analyse the metabolic profile of pDCs from SSc patients. Our results suggest that pDCs from ACA^+ patients rely more on oxidative phosphorylation (OXPHOS) and are more responsive to external stimuli, whereas pDCs from ATA^+ patients may exhibit a more activated or exhausted profile.

Keywords Systemic sclerosis, Scleroderma, Immunometabolism, Dendritic cells, Plasmacytoid dendritic cells

*Correspondence:
Catarina R. Almeida
cra@ua.pt

Full list of author information is available at the end of the article

Background

Systemic sclerosis (SSc) is a connective tissue disease characterised by immune dysregulation, vasculopathy and fibrosis of different organs [1]. SSc can be classified in two main subsets, based on the extent of skin involvement. In limited cutaneous SSc (lcSSc), fibrosis primarily affects the skin distal to the elbows or knees, whereas in diffuse cutaneous SSc (dcSSc), the involvement extends to the trunk [2, 3]. Additionally, most SSc patients exhibit at least one specific serum autoantibody, namely anti-centromere, anti-topoisomerase I and anti-RNA polymerase III antibodies (ACA, ATA, ARA respectively), which are associated with disease presentation and progression [2, 4]. ACA is typically associated with lcSSc, while ATA and ARA are more commonly found in dcSSc cases. Moreover, ATA^+ patients are more prone to developing lung fibrosis, leading to a less favourable prognosis, whereas ARA^+ patients often present renal crisis [2].

Plasmacytoid dendritic cells (pDCs) are professional type I interferon (IFN) producers involved in anti-viral responses, but also highly relevant for autoimmunity onset and flairs, particularly in diseases correlated with high IFN signature, such as SSc [5]. It has been reported that pDC numbers are increased in the skin and lung tissues of patients with SSc and decreased in circulation compared with healthy donors [6, 7]. Also, pDC depletion in mice models of SSc ameliorates fibrosis and inflammation, further underlining their participation in disease progression [6, 8]. pDCs can promote B cell activation and autoantibody production and secrete high levels of type I IFN and chemokine (C-X-C motif) ligand 4 (CXCL4), contributing to inflammation and fibrosis [7–11]. This situation is correlated with a dysregulation of the unfolded protein response (UPR) pathway inositol-requiring transmembrane kinase/endoribonuclease 1-alpha (IRE1α), that potentiates the tricarboxylic acid (TCA) cycle and was shown to contribute to the type I IFN signature observed in SSc patients [12].

Several immune cells, such as macrophages, dendritic cells (DCs), B cells and T cells, rely on metabolic reprogramming for differentiation and function [13]. Metabolic reprogramming of pDCs depends on the species and stimuli. Toll-like receptors (TLR)7/8-activated human pDCs were shown to upregulate oxidative phosphorylation (OXPHOS) dependently on glutaminolysis [14]. On the other hand, human pDCs stimulated with a TLR7 agonist, such as influenza A virus (IAV) or rhinovirus (RV), display increased glycolysis while OXPHOS was not impacted [15]. Other studies using mouse pDCs demonstrated that type I IFN derived from TLR9 activation contributes to fatty acid oxidation (FAO) and OXPHOS [16]. Most recently, it was proposed that chronic activation of pDCs in SSc could be due to dysregulation of metabolic pathways [12]. Nevertheless, the metabolic profile of these cells and its contribution to the disease's progression is unknown. Thus, this work aimed to gain insights into the metabolic profile of pDCs from patients with SSc. For that, we used SCENITH™, a single-cell technique that allows for the analysis of the metabolic profile of rare cell populations by flow cytometry, by assessing translation inhibition [17].

Methods

Patient inclusion and clinical data

Adult patients with SSc fulfilling the 2013 American College of Rheumatology/ European League Against Rheumatism classification criteria were included [4]. Patients with overlapping syndromes were not considered. All participants signed an informed consent form before inclusion and clinical data collected were anonymised. This study was approved by the Ethics Committee of Centro Hospitalar do Baixo Vouga (now ULS-RA) (Reference 44-069-2021).

Demographic, clinical and laboratory data were extracted from patients' medical records. Demographic information included gender, birth date, tobacco and alcohol use. Disease onset was defined as the time of the first occurrence of a non-Raynaud's symptom of SSc. Patients were categorised as lcSSc or dcSSc using LeRoy's criteria [18]. Clinical data included SSc-related symptoms and signs (Raynaud's phenomenon, digital ulcers, telangiectasia, puffy hands, sclerodactyly, calcinosis), modified Rodnan skin score (mRSS), and organ involvement. We used consensus definitions to characterise each major organ involvement of SSc, which were established in earlier studies [19]. We also included the nailfold videocapillaroscopy (NVC) pattern, and the ongoing treatments (glucocorticoids, immunomodulators, and vasodilators). Antinuclear autoantibodies (ANAs) were detected with an indirect immunofluorescence test (IIFT) on human epithelial cells (Hep-2) and anti–extractable nuclear antigen (ENA) analysis using the commercially available line immunoblot assay (EUROLINE Systemic Sclerosis (Nucleoli) Profile (IgG); Euroimmun, Lübeck, GER).

Cell isolation

Whole blood (20 mL) was collected in S-Monovette® Lithium Heparin (Sarstedt, Nümbrecht, GER) tubes, maintained at room temperature (RT) and processed within 1 h of venepuncture. Following blood centrifugation at 400 xg at RT for 10 min and plasma recovery, peripheral blood mononucleated cells (PBMCs) were isolated by density gradient centrifugation. Briefly, blood was diluted twice in PBS (Gibco, Thermo Fisher Scientific, Waltham, MA, USA), overlaid onto Ficoll-Paque Plus (Cytiva, Marlborough, MA, USA) and cells were separated by centrifugation at 400 xg for 10 min at 4 °C in a swinging bucket rotor without brake. The mononuclear

cell layer was transferred into a new tube, washed twice with PBS and finally with RPMI 1640 medium with 2 mM L-glutamine (Gibco).

Cell activation, SCENITH™ and pDC staining

To evaluate the metabolic profile of pDCs, we employed the flow cytometry based SCENITH™ method, which relies on the impact of metabolic pathway inhibition on protein synthesis levels to infer ATP and GTP availability [17]. SCENITH™ protocol was adapted from its previous description [17]. A scheme with the key steps of the protocol is presented in Fig. 1. Initially, 1.5×10^6 PBMCs were seeded in 170 µL RPMI 1640 with 2 mM L-glutamine (Gibco) supplemented with 10% heat-inactivated foetal bovine serum (FBS; Sigma-Aldrich, St. Louis, MO, USA) and 1% Penicillin-Streptomycin (Gibco) in a round-shaped bottom 96-well plate in the absence or presence of CpG A (3 µM; InvivoGen, San Diego, CA, USA) for 3 h. After activation, cells were treated for 40 min with vehicle control (C; DMSO), 2-deoxy-glucose (2-DG; 100 mM), oligomycin (O; 1 µM), a combination of 2-DG and O (DGO), and puromycin (10 µg/mL). As a negative control and 15 min before puromycin treatment, harringtonine (H) was added (2 µg/mL). After two washing steps with ice-cold FACS buffer (2% FBS, 2 µM EDTA, PBS) and before surface staining, cells were incubated for 15 min at 4 °C in the dark with a combination of Human TruStain FcX Fc Receptor Blocking Solution (BioLegend, San Diego, CA, USA) and Live/Dead™ (Invitrogen, Thermo Fisher Scientific). Surface staining with primary conjugated antibodies was performed for 25 min at 4 °C in the dark. After washing with FACS buffer, cells were fixed and permeabilised using Foxp3 Transcription Factor Staining Buffer Set (Invitrogen), according to the manufacturer's instructions. Cells were incubated for 10 min at RT with intracellular blocking solution (Foxp3 Permeabilization buffer (Invitrogen) with 20% FBS), and puromycin intracellular staining was performed for 1 h at 4 °C. After two washing steps with permeabilization buffer, cells were resuspended in FACS buffer.

The kit with SCENITH™ reagents (inhibitors, puromycin and anti-puromycin antibody) was from www.gammaomics.com. Information regarding the used antibodies is shown in Supplementary Table 1.

Data were acquired using BD Accuri C6 (BD Biosciences, San Jose, CA, USA). At least 300 $CD304^+$ Lin^- events were acquired per condition. Data were analysed using FlowJo™ v10.8.1 Software (BD Life Sciences, Franklin Lakes, NJ, USA) and were compensated using single stains with UltraComp eBeads™ Compensation Beads (ref. 01-2222-41, Invitrogen). The gating strategy is shown in Supplementary Fig. 1.

Glucose dependence, mitochondrial dependence, glycolytic capacity and fatty acid oxidation (FAO)/ amino acid oxidation (AAO) capacity were calculated as detailed below, using the median fluorescence intensities (MFI) of anti-puro-fluorochrome obtained upon treatment.

$$\text{Glucose dependence} = 100\left(\frac{\text{C - 2DG}}{\text{C - DGO}}\right)$$

$$\text{Mitochondrial dependence} = 100\left(\frac{\text{C - O}}{\text{C - DGO}}\right)$$

$$\text{Glycolytic capacity} = 100 - \text{Mitochondrial dependence}$$

$$\text{FAO/AAO capacity} = 100 \text{ - Glucose dependence}$$

Glucose and mitochondrial dependences give the proportion of translation dependent on glucose oxidation or OXPHOS, respectively [17]. Glycolytic capacity represents the maximum translation sustainability under mitochondrial respiration inhibition, while FAO and AAO capacity represents cell's ability to use fatty acids and amino acids as energy source when glucose oxidation is inhibited [17].

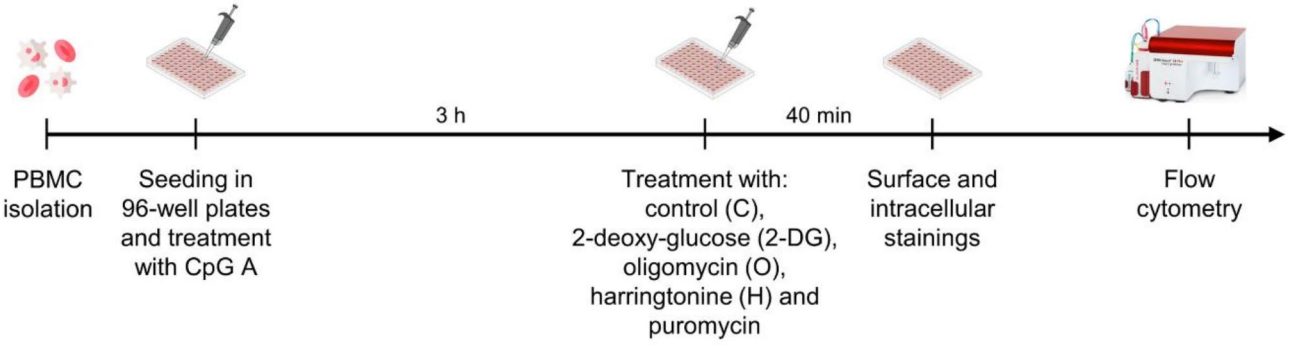

Fig. 1 Scheme representing the key steps of the methods used. PBMCs isolated from the blood of HCs and SSc patients were seeded in 96-well plates and treated with CpG A for 3 h, before 40-minute incubation with the SCENITH™ drugs – control (C), 2-deoxy-glucose (2-DG), oligomycin (O), harringtonine (H) and puromycin. Finally, stainings were performed and cells were analysed by flow cytometry

p-S6 staining

PBMCs were seeded, treated with CpG A and their surface stained as described for the SCENITH™ protocol. Cells were then stained for the intracellular phosphorylated form of ribosomal protein S6. Information about the used antibodies is in Supplementary Table 1.

Table 1 Participant demographics, clinical characteristics, and current therapies

Characteristic	SSc, *n* = 14	HCs, *n* = 10
Gender (%)		
Male	3 (21.4)	1 (10)
Female	11 (78.6)	9 (90)
Age (years)	56.5 (52.5–61.8)	49 (35.8–53.0)
Disease duration (years)	7.5 (3.8–10)	-
Limited cutaneous SSc (%)	8 (57.1)	-
Diffuse cutaneous SSc (%)	6 (42.9)	-
Raynaud's phenomenon (%)	14 (100)	-
DU (%)	8 (57.1)	-
Telangiectasias (%)	9 (64.3)	-
Puffy hands (%)	2 (14.3)	-
Sclerodactyly (%)	10 (71.4)	-
Calcinosis (%)	4 (28.6)	-
Arthralgias/Arthritis (%)	1 (7.1)	-
Myositis (%)	0 (0)	-
mRSS	11 (8–15)	-
ANA titre (%)		
1/320	2 (14.3)	-
1/640	6 (42.9)	-
1/1280	6 (42.9)	-
Presence of autoantibodies (%)		
ATA	6 (42.9)	-
ACA	4 (28.6)	-
ARA	4 (28.6)	
Organ complications (%)		
GI involvement	9 (69.2)	-
ILD	6 (46.2)	-
PAH	0	-
Cardiac involvement	0	-
NVC pattern (%)		
Early	6 (42.9)	-
Active	4 (28.6)	-
Late	3 (21.4)	-
Current therapies (%)		
Prednisolone	4 (30.8)	-
Methotrexate	4 (30.8)	-
Mycophenolate Mofetil	5 (38.5)	-
Nintedanib	2 (15.4)	-
Calcium antagonist	14 (100)	-

Median and IQR are reported unless otherwise stated. HC: healthy control; DU: digital ulcers; mRSS: modified Rodnan skin score; ANA: antinuclear antibody; ATA: anti-topoisomerase I antibody; ACA: anti-centromere antibody; ARA: anti-RNA polymerase III antibody; GI: gastrointestinal; ILD: interstitial lung disease; PAH: pulmonary arterial hypertension; NVC: nailfold videocapillaroscopy

Statistical analysis

Statistical analyses were performed using GraphPad Prism Software version 9.0.0 (GraphPad Software, Inc., La Jolla, CA, USA). Data are presented as median and interquartile range (IQR). The Shapiro-Wilk test was used to assess data normality and differences in variances were tested using F test. The most appropriate statistical test was then chosen according to each data set, as indicated in figure legends. $^{*}p \le 0.05$; $^{**}p \le 0.01$; $^{***}p \le 0.001$; $^{****}p \le 0.0001$.

Results

Study cohort characterisation

Fourteen SSc patients and ten healthy controls (HCs) were enrolled in this study (Table 1), with median ages of 56.5 (interquartile range, IQR 52.5–61.8) and 49 (IQR 35.8–53.0) years, respectively. Most were women (78.6% of SSc patients and 90% of HC). Median disease duration was 7.5 years (IQR 3.8–10). Eight patients (57.1%) presented lcSSc, and six (42.9%) presented dcSSc. Nine patients (69.2%) had gastrointestinal (GI) involvement (100% upper GI tract), and six (46.2%) presented interstitial lung disease (ILD). There were no patients with myositis, pulmonary arterial hypertension (PAH) or renal or cardiac involvement. Six patients (42.9%) were positive for ATA, four (28.6%) for ACA, and four (28.6%) for ARA. None of the patients was positive for more than one SSc-specific autoantibody. All patients were undergoing treatment, including immunosuppressants, antifibrotic agents and/or calcium antagonists.

The percentage of pDCs in circulation varies with ANA titre

Treatments were performed on the whole PBMC population, and pDCs were identified by flow cytometry as positive for the pDC marker CD304 (also known as BDCA4) and negative for CD3, CD14, CD16, CD19, CD20, CD34 and CD56 (Lin^-) (Fig. 2A, gating strategy presented in Supplementary Fig. 1A). It was confirmed that $CD304^+$ cells are also positive for the pDC markers CD123 and HLA-DR, while events positive for these pDC markers are also Lin^- (Fig. 1B, C).

No statistically significant differences were found in the percentage of pDCs in circulation among HCs and patients with lcSSc or dcSSc (Fig. 2B). Similarly, no significant differences were observed when stratifying patients by the presence or absence of digital ulcers (DU), telangiectasias, sclerodactyly, calcinosis, ILD, GI involvement or by disease duration (Fig. 2C-I). However, patients with an ANA titre of 1/1280 exhibited a reduced percentage of pDCs among PBMCs compared to those with an ANA titre of 1/640 (Fig. 2J), while no significant differences were found comparing patients positive for different SSc-specific autoantibodies (Fig. 2K).

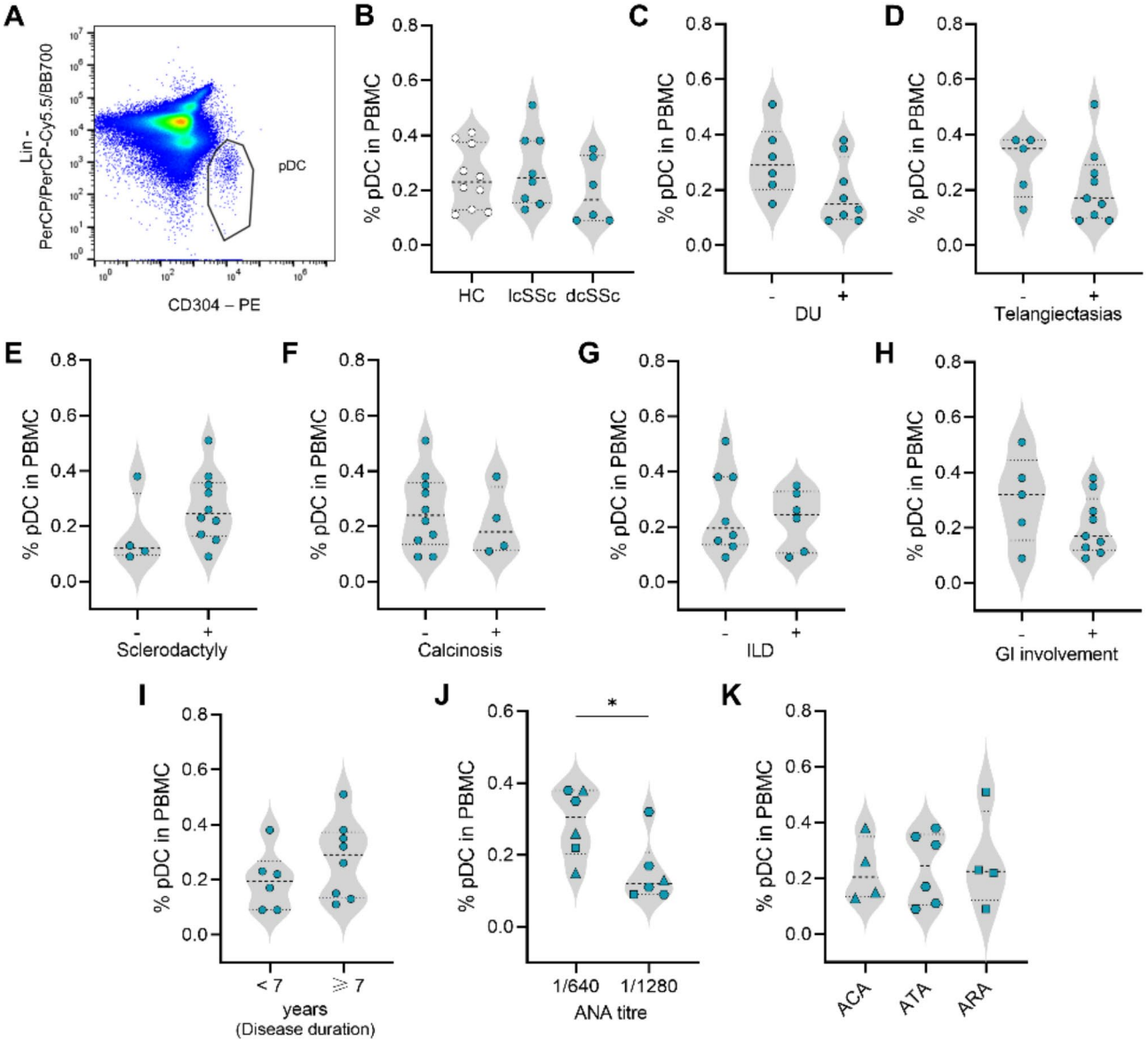

Fig. 2 The percentage of circulating pDCs in SSc patients changes with progression of the disease. **(A)** Identification of $CD304^{+}$ Lin^{-} pDCs by flow cytometry. **(B-K)** The percentage of pDCs was obtained by flow cytometry analysis and comparisons were performed between patient groups. Data are expressed as median and IQR and each dot represents data from one donor. One-way ANOVA followed by Tukey's multiple comparisons test (B, K) or unpaired *t* test (C-J), except for (E) where Mann-Whitney was performed. *$p \leq 0.05$

pDCs present a similar metabolic profile in SSc and HCs

Inhibition of glycolysis and OXPHOS by 2-deoxy-glucose (2-DG) and oligomycin (O), respectively, led to a reduction in translation to levels similar to harringtonine (H), a protein synthesis inhibitor (Fig. 3A, B). This shows that pDCs are susceptible to metabolic modulation and rely on both glycolysis and OXPHOS for protein synthesis, measured by puromycilation detection and used as a read-out for ATP and GTP availability. Under basal conditions, pDCs from HCs and SSc patients showed similar translation and S6 phosphorylation levels (Fig. 3C, D). As expected, it was possible to activate TLR9 by stimulation with CpG A, which led to increased levels of phosphorylated S6 in both HCs and SSc patients, even though statistical significance is only observed for the latter (Fig. 3D). However, treatment with CpG A did not affect protein synthesis on pDCs, nor their response to metabolic modulation (Fig. 3A-C). Moreover, the metabolic profile of pDCs was not affected by TLR9 activation and seemed comparable under both SSc and healthy conditions (Fig. 3E, F). Given the lack of differences upon TLR9 stimulation, the follow-up analysis on the metabolic profile of pDCs was focused on cells in basal conditions.

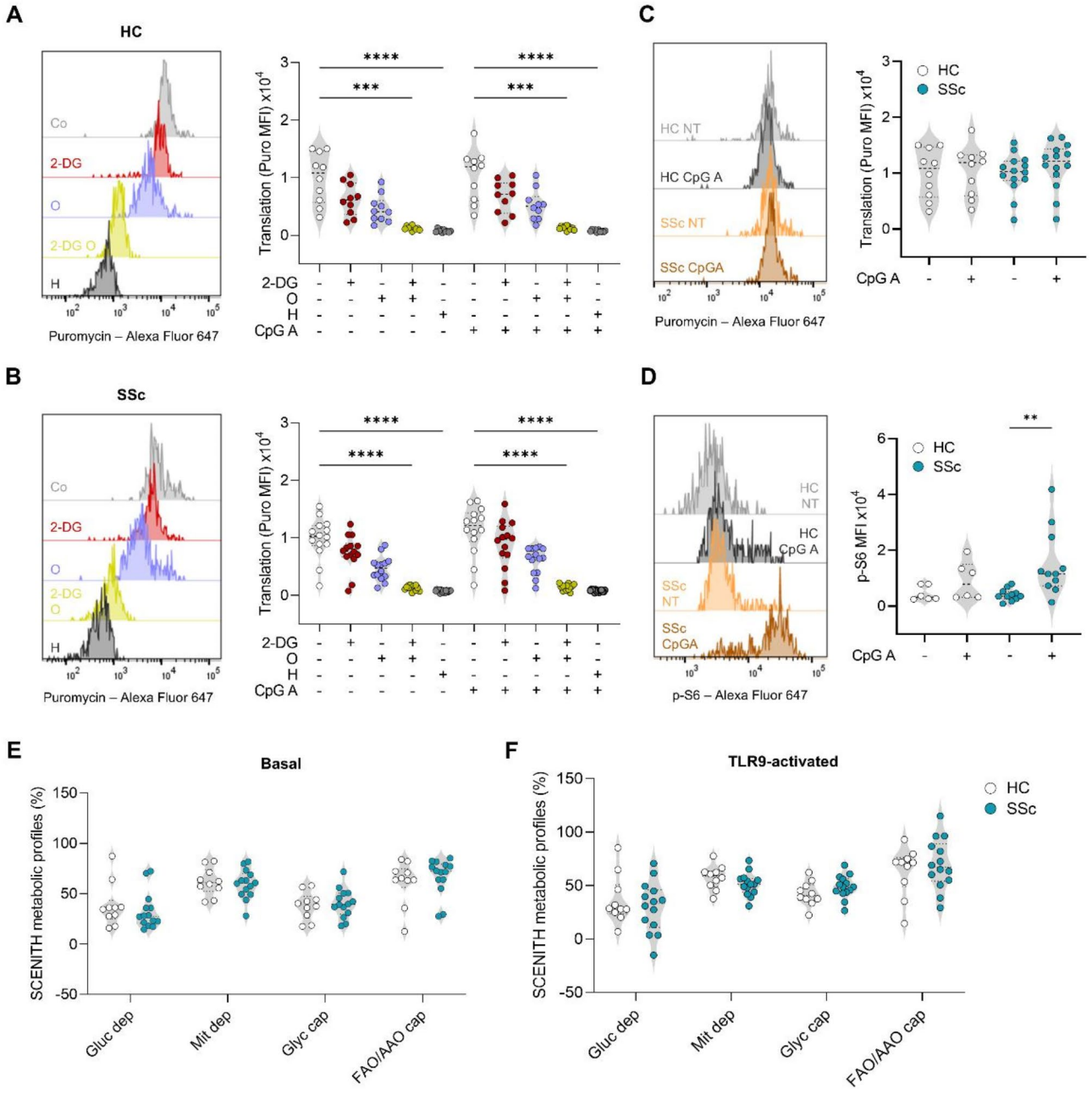

Fig. 3 pDCs from HCs and SSc patients have no major differences in their metabolic profile. **(A**, **B)** Translation levels in pDCs after treatment with 2-deoxy-glucose (2-DG), oligomycin (O), harringtonine (H) and CpG A. Representative histograms for cells not TLR9-activated. **(C)** Translation and **(D)** S6 phosphorylation (MFI) levels. **(E**, **F)** SCENITH™ metabolic profiles. Data expressed as median and IQR; dots represent independent donors. Kruskal-Wallis test followed by Dunnet's multiple comparisons test (A, B), one-way ANOVA followed by Sidak's multiple comparisons test (C, D) and two-way ANOVA followed by Sidak's multiple comparisons test (E, F) were used. $^{**}p \leq 0.01$; $^{***}p \leq 0.001$; $^{****}p \leq 0.0001$

pDCs from ACA and ATA-positive patients have different metabolic profiles

During our analysis we noted potential differences among groups of SSc patients and decided to segregate patients according to their clinical characteristics. pDCs from lcSSc patients display higher upregulation of S6 phosphorylation and protein synthesis after treatment with CpG A, in comparison with cells from dcSSc patients, suggesting higher sensitivity to TLR9 stimulation (Fig. 4A, B). There was also a significant decrease in the basal levels of translation associated with presence of digital ulcers (DU) and GI involvement but not with the presentation of telangiectasias, sclerodactyly, calcinosis, ILD, disease duration or ANA titre (Supplementary Fig. 2). However, at basal conditions, no differences were found in the metabolic profile of cells isolated from

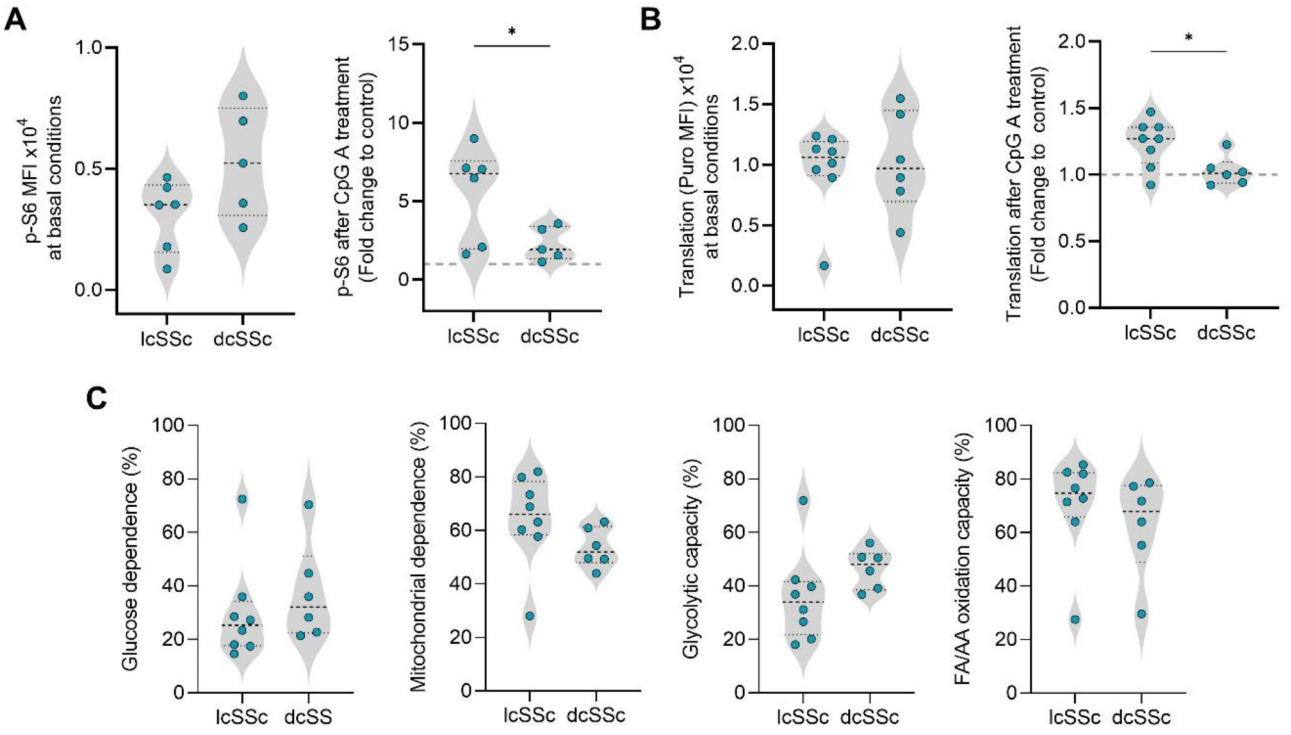

Fig. 4 pDCs from lcSSc patients are more reactive to CpG A than cells from dsSSc. **(A)** p-S6 levels and **(B)** translation levels at basal and TLR9-activated conditions were assessed in pDC from SSc patients by flow cytometry. **(C)** Metabolic profiles. Dash line corresponds to 1. Data are expressed as median and IQR and each dot represents data from one donor. Statistical significance was tested with unpaired *t* test (A, B-right, C-mitochondrial dependence and glycolytic capacity) or Mann-Witney test (B-left, C-glucose dependence and FA/AA oxidation capacity). *$p \leq 0.05$

lcSSc or dcSSc (Fig. 4C), as well as among patients stratified accordingly to the presence of DU, telangiectasias, sclerodactyly, calcinosis, ANA titre, disease duration, GI involvement or presentation of ILD (Supplementary Fig. 3).

On the other hand, pDCs from ACA$^+$ patients exhibited higher mitochondrial dependence and lower glycolytic capacity compared to cells from ATA$^+$ patients (Fig. 5A). Moreover, pDCs from ACA$^+$ patients showed an upregulation of translation levels after TLR9 stimulation, compared to ATA$^+$ and ARA$^+$ patients (Fig. 5B). There were no statistically significant differences on levels of p-S6, but there was a tendency for pDCs from ARA$^+$ patients to display higher p-S6 levels at basal conditions (Fig. 5C). Characteristics of ATA-, ACA- and ARA-positive patients are summarized in Table 2. Together, these data suggest that pDCs from ACA$^+$ patients rely more on OXPHOS and are more responsive to external stimuli.

Discussion

The key role of pDCs in SSc pathophysiology has been highlighted by others [6–12]. As with other immune cells, pDCs heavily rely on metabolic reprogramming for their differentiation and function [20, 21]. A reduced expression of phosphoglycerate dehydrogenase (PHGDH) in pDCs isolated from the blood of SSc patients, and the downregulation of interferon-stimulated genes (ISGs) expression upon TCA cycle inhibition were recently reported [12]. Nevertheless, the metabolic profile of pDCs in SSc has not been characterised. In this study, we show how to use SCENITH™, a single-cell resolution method that employs flow cytometry analysis of protein synthesis, to infer the metabolic profile of these cells [17]. Due to the importance of cell activation in this context, we analysed both cells at basal conditions and pre-treated with CpG A, a TLR9 agonist. Treatments were performed in the whole PBMC population, and the analysis focused on CD304$^+$ Lin$^-$ cells.

The activation state of pDCs was evaluated by analysing p-S6 levels, whose levels increase upon activation of the PI3K-PKB-mTOR pathway, functioning as a marker of TLR9 activation [22], and by monitoring protein synthesis, which is reported to increase during immune cell activation to sustain cellular function [23–25]. Globally, pDCs from HCs and SSc patients seemed to have the same basal activation state since no differences in p-S6 and translation levels were found. However, pDCs from ACA$^+$ patients upregulated their translation levels in response to TLR9 activation, contrary to what happens with ATA$^+$ or ARA$^+$ patients. A higher increase in translation upon TLR9 activation was also observed in lcSSc, compared to dcSSc. Although not statistically significant,

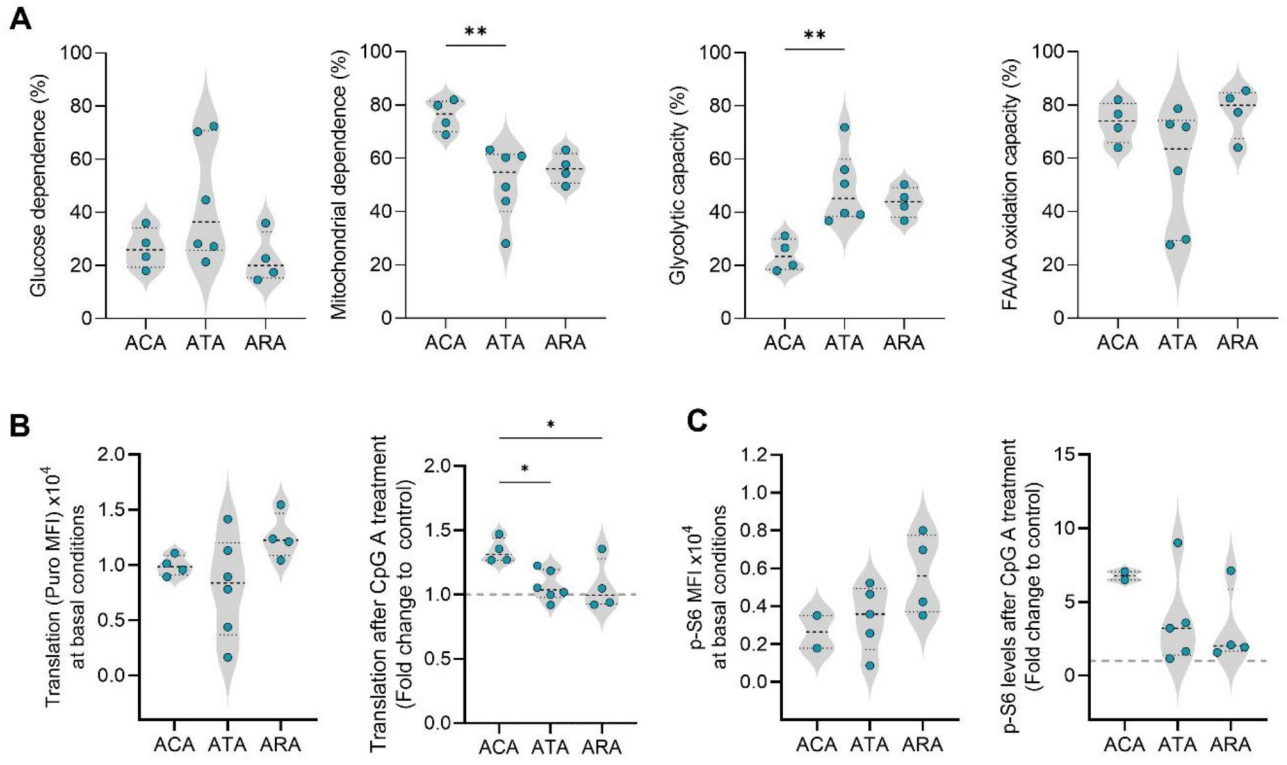

Fig. 5 pDCs from ACA$^+$ patients are more dependent on mitochondrial metabolism and have lower glycolytic capacity than cells from ATA$^+$ patients. (**A**) SCENITH™ metabolic profiles, (**B**) translation levels, and (**C**) p-S6 levels were determined by flow cytometry for pDCs from patients with different patterns of SSc autoantibodies. Data are expressed as median and IQR and each dot represents data from one donor. Kruskal-Wallis test followed by Dunnet's multiple comparisons test was used for (**A**), one-way ANOVA followed by Tukey's multiple comparisons test for (**B**) and one-way ANOVA followed by Sidak's multiple comparisons test for (**C**). *$p \leq 0.05$, **$p \leq 0.01$

there was a tendency for pDCs from dcSSc and patients positive for ATA or ARA to present increased p-S6 at basal conditions. Together, these data suggest that pDCs from dcSSc and ATA$^+$ and ARA$^+$ patients have basal activation, which might limit the effect of CpG A.

Even though the treatment with CpG A induced S6 phosphorylation, it did not upregulate translation, nor impact the metabolic profile of these cells. Other studies have observed an impact of TLR9 activation in the metabolism of pDCs [16, 26], but longer exposure times to the agonist were used. As mentioned above, a more recent study exploring the metabolism of pDCs from SSc patients used a similar timepoint and analysed the expression of an enzyme involved in the biosynthesis of serine [12]. Therefore, differences from what is reported in the literature may be due to differences in the agonist and stimulation times used.

Interestingly, although pDCs from HCs and SSc patients displayed similar metabolic profiles, being dependent on both glycolysis and OXPHOS, variations were found among patients positive for the different ANAs subtypes. While there were no differences in the activation or metabolic state of pDCs from ATA$^+$ and ARA$^+$ patients, pDCs from ACA$^+$ patients presented higher mitochondrial dependence and lower glycolytic capacity than those from ATA$^+$ patients. This suggests that pDCs from ACA$^+$ patients rely more on OXPHOS for energy production. On the other hand, cells from ATA$^+$ patients tended to be more dependent on glycolysis. Usually, activated immune cells and highly proliferating cells shift their metabolism to glycolysis, while OXPHOS is preferred at the resolution phase [27]. Thus, the metabolic profile results are concordant with p-S6 readouts and suggest that pDCs from ATA$^+$ patients are more activated, relying on glycolysis for energy production. The interaction between autoantibodies and soluble antigens can form immune complexes (ICs), promoting cell activation, namely in SSc [20–31]. Thus, it will be interesting to clarify in future studies if the differences in the metabolic profile of pDCs are related to their activation by ICs.

The identification of pDCs by flow cytometry as CD304$^+$ Lin$^-$ (CD3, CD14, CD16, CD19, CD20, CD34 and CD56) can be viewed as a possible limitation of this work. Even though we confirmed that these cells were also positive for other pDC markers (CD123 and HLA-DR), we cannot certainly exclude a low percentage contamination by other cells. Moreover, these findings are in

Table 2 Demographics, clinical characteristics, and current therapies of ATA-, ACA- and ARA-positive patients

Characteristic	ACA$^+$, $n=4$	ATA$^+$, $n=6$	ARA$^+$, $n=4$
Gender (%)			
Male	0 (0)	3 (50)	0 (0)
Female	4 (100)	3 (50)	4 (100)
Age (years)	64.5 (35.8–70.8)	54.5 (50.8–57.8)	55.5 (53.3–64.5)
Disease duration (years)	10 (7.8–10.8)	6 (2.8–10.8)	4 (3.3–8.5)
Limited cutaneous SSc (%)	4 (100)	2 (33.3)	2 (50)
Diffuse cutaneous SSc (%)	0 (0)	4 (66.7)	2 (50)
Raynaud's phenomenon (%)	4 (100)	6 (100)	4 (100)
DU (%)	2 (50)	4 (66.7)	2 (50)
Telangiectasias (%)	2 (50)	4 (66.7)	3 (75)
Puffy hands (%)	1 (25)	0 (0)	2 (50)
Sclerodactyly (%)	3 (75)	4 (66.7)	3 (75)
Calcinosis (%)	2 (50)	1 (16.7)	1 (25)
Arthralgias/Arthritis (%)	0 (0)	1 (16.7)	0 (0)
Myositis (%)	0 (0)	0 (0)	0 (0)
mRSS	12.5 (2.5–15)	12.5 (8.8–25.8)	10 (4.0-11.5)
ANA titre (%)			
1/320	0 (0)	0 (0)	2 (50)
1/640	3 (75)	2 (33.3)	1 (25)
1/1280	1 (25)	4 (66.7)	1 (25)
Organ complications (%)			
GI involvement	4 (100)	4 (66.7)	1 (25)
ILD	1 (25)	4 (66.7)	1 (25)
PAH	0 (0)	0 (0)	0 (0)
Cardiac involvement	0 (0)	0 (0)	0 (0)
NVC pattern (%)			
Early	1 (25)	2 (33.3)	3 (75)
Active	2 (50)	2 (33.3)	0 (0)
Late	1 (25)	2 (33.3)	0 (0)
Current therapies (%)			
Immunosuppressants (prednisolone, methotrexate and/or mycophenolate mofetil)	2 (50)	4 (66.7)	2 (50)
Antifibrotics	0 (0)	2 (33.3)	0 (0)
Vasodilators	4 (100)	6 (100)	4 (100)

Median and IQR are reported unless otherwise stated. HC: healthy control; DU: digital ulcers; mRSS: modified Rodnan skin score; ANA: antinuclear antibody; ATA: anti-topoisomerase I antibody; ACA: anti-centromere antibody; ARA: anti-RNA polymerase III antibody; GI: gastrointestinal; ILD: interstitial lung disease; PAH: pulmonary arterial hypertension; NVC: nailfold videocapillaroscopy

circulating pDCs, which may not be the cell population with the highest influence on the disease course. Infiltrating pDCs likely have a more prominent role in SSc pathogenesis. However, as SSc is a systemic disease, it is also possible that the profile of circulating pDCs reflects what happens in the affected tissues. Additionally, the analysed patients were undergoing therapy at the time of sampling, with treatments lasting for at least one year. More than half of the patients were receiving immunosuppressive therapies, whose impact on the metabolic profile of pDCs remains undetermined. Finally, our analyses were performed with a low number of cells and patients, inherent to the challenges posed by the rarity of this cell population and the disease, and other methods could be used to check cell activation (e.g. expression of IFN and ISGs). Despite these limitations, this study shows how to apply a single cell flow cytometry-based methodology (SCENITH™) to analyse the metabolic profile of cells traditionally difficult to study, providing valuable information on the pathophysiology of SSc. Moreover, the sex and age distribution of the patients included reflects the Portuguese SSc patients' demographics [32], adding relevance to our findings.

Overall, we found that pDCs from ACA$^+$ patients had reduced glycolytic capacity, associated with a stronger response to in vitro TLR9 activation, comparing with ATA$^+$ patients. Whether these differences are a cause or a consequence of disease severity and clinical progression of SSc remains to be clarified. Future studies, including validating these findings in larger cohorts and testing the impact of blocking glycolysis while promoting mitochondrial respiration on pDC, may contribute to defining new possible therapeutic strategies for SSc.

Conclusions

In summary, our findings suggest that the metabolic profile of pDCs is correlated with the severity and progression of SSc. Specifically, pDCs from ACA$^+$ patients have a higher dependence on mitochondrial respiration and lower reliance on glycolysis, appearing to be less activated at basal conditions. These results contribute to the understanding of SSc pathophysiology and highlight the potential of single cell flow cytometry analyses to study the metabolic profile of rare cell populations in SSc.

Abbreviations

2-DG	2-deoxy-glucose
AAO	Amino acid oxidation
ACA	Anti-centromere antibody
ANA	Antinuclear autoantibody
ARA	Anti-RNA polymerase III antibody
ATA	Anti-topoisomerase antibody
CXCL4	Chemokine (C-X-C motif) ligand 4
DC	Dendritic cell
dcSSc	Diffuse cutaneous systemic sclerosis
DU	Digital ulcers
ENA	Extractable nuclear antigen
FAO	Fatty acid oxidation
FAO	Fatty acid oxidation
GI	Gastrointestinal
HC	Healthy control
IAV	Influenza A virus
IC	Immune complex
IFN	Interferon
IIFT	Indirect immunofluorescence test
ILD	Interstitial lung disease

IQR	Interquartile range
IRE1α	Inositol-requiring transmembrane kinase/endoribonuclease 1-alpha
ISG	Interferon-stimulated gene
lcSSc	Limited cutaneous systemic sclerosis
MFI	Median fluorescence intensities
mRSS	Modified Rodnan skin score
NVC	Nailfold videocapillaroscopy
OXPHOS	Oxidative phosphorylation
PAH	Pulmonary arterial hypertension
PBMC	Peripheral blood mononuclear cells
pDC	Plasmacytoid dendritic cell
PHGDH	Phosphoglycerate dehydrogenase
RT	Room temperature
RV	Rhinovirus
SSc	Systemic sclerosis
SSc-IC	IC containing antibodies specific for SSc
TCA	Tricarboxylic acid
TLR	Toll-like receptor
UPR	Unfolded protein response

Supplementary Information

The online version contains supplementary material available at https://doi.org/10.1186/s13075-025-03500-3.

Supplementary Material 1

Acknowledgements

We thank all the volunteers, especially the patients, and the health professionals (Anabela Barcelos, Maria do Céu Morais, Graça Costa, António José Oliveira) involved in this study.

Author contributions

BHF: Conceptualization, Data curation, Formal analysis, Investigation, Methodology, Visualization, Writing – original draft, Writing – review and editing. CM: Conceptualization, Data curation, Investigation, Methodology, Resources, Writing – review and editing. ED: Data curation, Methodology, Writing – review and editing. JLS: Investigation, Methodology, Resources, Writing – review and editing. ARP: Data curation, Methodology, Writing – review and editing. RJA: Methodology, Resources, Writing – review and editing. IFD: Funding acquisition, Methodology, Supervision, Writing – review and editing. PP: Funding acquisition, Methodology, Supervision, Writing – review and editing. CRA: Conceptualization, Funding acquisition, Investigation, Methodology, Project administration, Supervision, Writing – original draft, Writing – review and editing.

Funding

This work was supported by the World Scleroderma Foundation and Edith Busch Stiftung (the EBF and WSF Research Grant Programme 2022–2023). Work developed within the scope of iBiMED – Institute of Biomedicine (references UIDB/04501/2020, DOI https://doi.org/10.54499/UIDB/04501/2020, UIDP/04501/2020, DOI https://doi.org/10.54499/UIDP/04501/2020), CICECO – Aveiro Institute of Materials (UIDB/50011/2020, DOI https://doi.org/10.54499/UIDB/50011/2020; UIDP/50011/2020, DOI https://doi.org/10.54499/UIDP/50011/2020 & LA/P/0006/2020, DOI https://doi.org/10.54499/LA/P/0006/2020), and LAQV-REQUIMTE (LA/P/0008/202, DOI https://doi.org/10.54499/LA/P/0008/2020; UIDP/50006/2020, DOI https://doi.org/10.54499/UIDP/50006/2020; UIDB/50006/2020, DOI10.54499/UIDB/50006/2020) and the project with the reference 2022.03217.PTDC (DOI https://doi.org/10.54499/2022.03217.PTDC), financially supported by national funds (OE), through Fundação para a Ciência e a Tecnologia (FCT)/MCTES. FCT is also acknowledged for the individual grant to B.H.F. (SFRH/BD/144706/2019; DOI https://doi.org/10.54499/SFRH/BD/144706/2019) and the research contract under the Scientific Employment Stimulus to I.F.D. (CEECIND/02387/2018).

Data availability

The datasets generated and/or analysed during the current study are available upon reasonable request.

Declarations

Ethics approval and consent to participate

All participants signed an informed consent form before inclusion and clinical data collected were anonymised. This study was approved by the Ethics Committee of Centro Hospitalar do Baixo Vouga (now ULS-RA) (Reference 44-069-2021).

Consent for publication

Not applicable.

Competing interests

Rafael J. Argüello is scientist and co-founder of GammaOmics, a startup that holds the exclusive license to commercialize and provide services for SCENITH™, a technology utilized in this study. No other conflicts of interest are declared.

Author details

[1]Institute of Biomedicine (iBiMED), Department of Medical Sciences, University of Aveiro, Aveiro, Portugal
[2]Department of Chemistry, CICECO - Aveiro Institute of Materials, University of Aveiro, Aveiro, Portugal
[3]Rheumatology Department, Unidade Local de Saúde da Região de Aveiro, Aveiro, Portugal
[4]Aveiro Rheumatology Research Centre, Egas Moniz Health Alliance, Aveiro, Portugal
[5]EpiDoc Unit, Nova Medical School, NOVA University Lisbon, Lisboa, Portugal
[6]Rheumatology Research Unit, Faculdade de Medicina, Instituto de Medicina Molecular, Universidade de Lisboa, Lisboa, Portugal
[7]School of Health Sciences (ESSUA), University of Aveiro, Aveiro, Portugal
[8]Centre d'Immunologie de Marseille-Luminy, Aix Marseille Université, CNRS, INSERM, Marseille, France
[9]GammaOmics, Marseille, France
[10]Department of Chemistry, LAQV-REQUIMTE, University of Aveiro, Aveiro, Portugal
[11]Shanghai Institute of Immunology, Department of Microbiology and Immunology, Shanghai Jiao Tong University School of Medicine, Shanghai 200025, PR China

Received: 6 December 2024 / Accepted: 6 February 2025
Published online: 19 February 2025

References

1. Volkmann ER, Andréasson K, Smith V. Systemic sclerosis. Lancet. 2022;401:304–18.
2. Denton CP, Khanna D. Systemic sclerosis. Lancet. 2017;390:1685–99.
3. Clark KEN, Campochiaro C, Host LV, Sari A, Harvey J, Denton CP, et al. Combinations of scleroderma hallmark autoantibodies associate with distinct clinical phenotypes. Sci Rep. 2022;12:11212.
4. Van Den Hoogen F, Khanna D, Fransen J, Johnson SR, Baron M, Tyndall A, et al. 2013 classification criteria for systemic sclerosis: an American college of rheumatology/European league against rheumatism collaborative initiative. Ann Rheum Dis. 2013;72(11):1747–55.
5. Silva IS, Ferreira BH, Almeida CR. Molecular mechanisms behind the role of Plasmacytoid dendritic cells in systemic sclerosis. Biology (Basel). 2023;12:285.
6. Kafaja S, Valera I, Divekar AA, Saggar R, Abtin F, Furst DE, et al. pDCs in lung and skin fibrosis in a bleomycin-induced model and patients with systemic sclerosis. JCI Insight. 2018;3(9):e98380.
7. Ah Kioon MD, Tripodo C, Fernandez D, Kirou KA, Spiera RF, Crow MK, et al. Plasmacytoid dendritic cells promote systemic sclerosis with a key role for TLR8. Sci Transl Med. 2018;10:eaam8458.
8. Ross RL, Corinaldesi C, Migneco G, Carr IM, Antanaviciute A, Wasson CW, et al. Targeting human plasmacytoid dendritic cells through BDCA2 prevents skin inflammation and fibrosis in a novel xenotransplant mouse model of scleroderma. Ann Rheum Dis. 2021;80(7):920–9.
9. Van Bon L, Affandi AJ, Broen J, Christmann RB, Marijnissen RJ, Stawski L, et al. Proteome-wide analysis and CXCL4 as a biomarker in systemic sclerosis. N Engl J Med. 2014;370(5):433–43.

10. Lande R, Lee EY, Palazzo R, Marinari B, Pietraforte I, Santos GS, et al. CXCL4 assembles DNA into liquid crystalline complexes to amplify TLR9-mediated interferon-α production in systemic sclerosis. Nat Commun. 2019;10(1):1731.
11. Lande R, Mennella A, Palazzo R, Pietraforte I, Stefanantoni K, Iannace N, et al. Anti-CXCL4 antibody reactivity is present in systemic sclerosis (SSc) and correlates with the SSc type I interferon signature. Int J Mol Sci. 2020;21(14):1–16.
12. Chaudhary V, Ah Kioon MD, Hwang SM, Mishra B, Lakin K, Kirou KA, et al. Chronic activation of pDCs in autoimmunity is linked to dysregulated ER stress and metabolic responses. J Exp Med. 2022;219(11):e20221085.
13. O'Neill LAJ, Kishton RJ, Rathmell J. A guide to immunometabolism for immunologists. Nat Rev Immunol. 2016;16(9):553–65.
14. Basit F, Mathan T, Sancho D, De Vries JM. Human dendritic cell subsets undergo distinct metabolic reprogramming for immune response. Front Immunol. 2018;9:2489.
15. Bajwa G, DeBerardinis RJ, Shao B, Hall B, Farrar JD, Gill MA. Cutting Edge: critical role of glycolysis in human plasmacytoid dendritic cell antiviral responses. J Immunol. 2016;196(5):2004–9.
16. Wu D, Sanin DE, Everts B, Chen Q, Qiu J, Buck MD, et al. Type 1 interferons induce changes in Core Metabolism that are critical for Immune function. Immunity. 2016;44(6):1325–36.
17. Argüello RJ, Combes AJ, Char R, Gigan J-P, Baaziz AI, Bousiquot E, et al. SCENITH: a Flow Cytometry-based method to functionally Profile Energy metabolism with single-cell resolution. Cell Metab. 2020;32(6):1063–e10757.
18. LeRoy EC, Black C, Fleischmajer R, Jablonska S, Krieg T, Medsger TA Jr, et al. Scleroderma (systemic sclerosis): classification, subsets and pathogenesis. J Rheumatol. 1988;15(2):202–5.
19. Nihtyanova SI, Sari A, Harvey JC, Leslie A, Derrett-Smith EC, Fonseca C, et al. Using autoantibodies and cutaneous subset to develop outcome-based Disease classification in systemic sclerosis. Arthritis Rheumatol. 2020;72(3):465–76.
20. He Z, Zhu X, Shi Z, Wu T, Wu L. Metabolic regulation of dendritic cell differentiation. Front Immunol. 2019;10:410.
21. Saas P, Varin A, Perruche S, Ceroi A. Recent insights into the implications of metabolism in plasmacytoid dendritic cell innate functions: potential ways to control these functions. F1000Res. 2017;6:456.
22. Combes A, Camosseto V, N'Guessan P, Argüello RJ, Mussard J, Caux C, et al. BAD-LAMP controls TLR9 trafficking and signalling in human plasmacytoid dendritic cells. Nat Commun. 2017;8(1):913.
23. Kelly B, Pearce EL. Amino assets: how amino acids support immunity. Cell Metab. 2020;32(2):154–75.
24. Pierre P. Immunity and the regulation of protein synthesis: surprising connections. Curr Opin Immunol. 2009;21(1):70–7.
25. Lelouard H, Schmidt EK, Camosseto V, Clavarino G, Ceppi M, Hsu H-T, et al. Regulation of translation is required for dendritic cell function and survival during activation. J Cell Biol. 2007;179(7):1427–39.
26. Fekete T, Sütö MI, Bencze D, Mázló A, Szabo A, Biro T, et al. Human plasmacytoid and monocyte-derived dendritic cells display distinct metabolic Profile upon RIG-I activation. Front Immunol. 2018;9:3070.
27. Soto-Heredero G, Gómez de las Heras MM, Gabandé-Rodríguez E, Oller J, Mittelbrunn M. Glycolysis – a key player in the inflammatory response. FEBS J. 2020;287(16):3350–69.
28. Raschi E, Chighizola CB, Cesana L, Privitera D, Ingegnoli F, Mastaglio C, et al. Immune complexes containing scleroderma-specific autoantibodies induce a profibrotic and proinflammatory phenotype in skin fibroblasts. Arthritis Res Ther. 2018;20(1):1–18.
29. Raschi E, Privitera D, Bodio C, Lonati PA, Borghi MO, Ingegnoli F, et al. Scleroderma-specific autoantibodies embedded in immune complexes mediate endothelial damage: an early event in the pathogenesis of systemic sclerosis. Arthritis Res Ther. 2020;22(1):265.
30. Eloranta ML, Franck-Larsson K, Lövgren T, Kalamajski S, Rönnblom A, Rubin K, et al. Type I interferon system activation and association with disease manifestations in systemic sclerosis. Ann Rheum Dis. 2010;69(7):1396–402.
31. Kim D, Peck A, Santer D, Patole P, Schwartz SM, Molitor JA, et al. Induction of interferon-α by scleroderma sera containing autoantibodies to topoisomerase I: Association of higher interferon-α activity with lung fibrosis. Arthritis Rheum. 2008;58(7):2163–73.
32. Freitas R, Martins P, Dourado E, Santiago T, Guimarães F, Fernandes BM, et al. Clinical features and outcome of 1054 patients with systemic sclerosis: analysis of Reuma.pt/SSc registry. ARP Rheumatol. 2022;1(1):21–9.

Publisher's note